ACS OMEGA

http://pubs.acs.org/journal/acsodf

Article

New Formulation to Accelerate the Degradation of Pesticide Residues: Composite Nanoparticles of Imidacloprid and 24-Epibrassinolide

Jingyu Zhao, Rong Song,* Hui Li, Qianqi Zheng, Shaomei Li, Lejun Liu, Xiaogang Li, Lianyang Bai, and Kailin Liu*

Cite This: *ACS Omega* 2022, 7, 29027−29037

Read Online

ACCESS | Metrics & More | Article Recommendations | Supporting Information

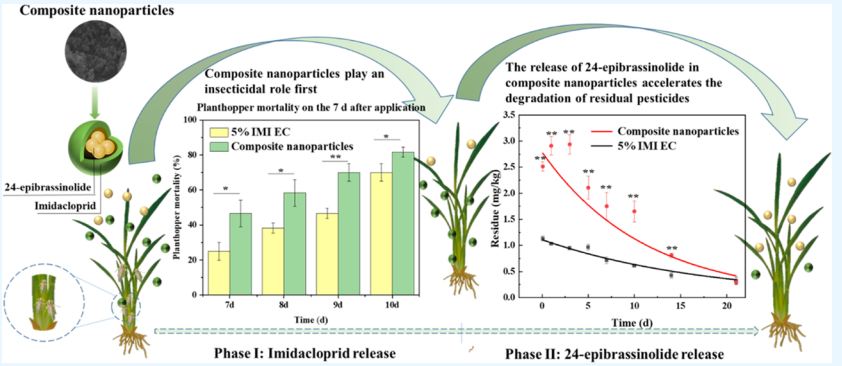

ABSTRACT: Pest control effectiveness and residues of pesticides are contradictory concerns in agriculture and environmental conservation. On the premise of not affecting the insecticidal effect, the pesticide residues in the later stage should be degraded as fast as possible. In the present study, composite nanoparticles in a double-layer structure, consisting of imidacloprid (IMI) in the outer layer and plant hormone 24-epibrassinolide (24-EBL) in the inner layer, were prepared by the W/O/W solvent evaporation method using Eudragit RL/RS and polyhydroxyalkanoate as wall materials. The release of IMI in the outer layer was faster and reached the maximum within 24 h, while the release of 24-EBL in the inner layer was slower and reached the maximum within 96 h. The contact angle of the composite nanoparticles was half that of the 5% IMI emulsifiable concentrate (EC), and the deposition of composite nanoparticles on rice was twice that of 5% IMI EC, which increased the pesticide utilization efficiency. Compared with the common pesticide, 5% IMI EC, the insecticidal effect of the composite nanoparticles was stronger than that of planthoppers, with a much lower final residue amount on rice after 21 days. The composite nanoparticles prepared in this study to achieve sustained release of pesticides and, meanwhile, accelerate the degradation of pesticide residues have a strong application potential in agriculture for controlling pests and promoting crop growth.

1. INTRODUCTION

Pesticides, as chemical agents for controlling pests and promoting plant growth, play a major role in meeting the food demand of the world's growing population.[1,2] However, the toxicity of pesticides leads to enormous adverse effects on human health and the environment.[3,4] Numerous studies have shown that during applications, less than 0.1% of the conventional pesticide active ingredients are effective on the target pests, and a large proportion of pesticides lead to serious residue problems.[5,6]

Plenty of biotic and abiotic degradation technologies have been developed to degrade pesticide residues.[7] Biodegradation includes direct and indirect strategies. Direct biodegradation is mainly through the decomposition and utilization of pesticides by pesticide-degrading microorganisms.[8] Indirect biodegradation uses certain hormones or endophytes to induce the activity of plant detoxification enzymes.[9] Abiotic degradation includes photolysis and hydrolysis.[7] At present, these degradation techniques are often used when pesticide residues occur, making it difficult for the degradation agent to interact with the pesticide.

Some new sustained-release pesticide formulations have been introduced to agricultural application to increase the effective period of pesticides.[10] However, these sustained-release pesticide formulations also enhance the risk of pesticide

Received: May 6, 2022
Accepted: August 1, 2022
Published: August 12, 2022

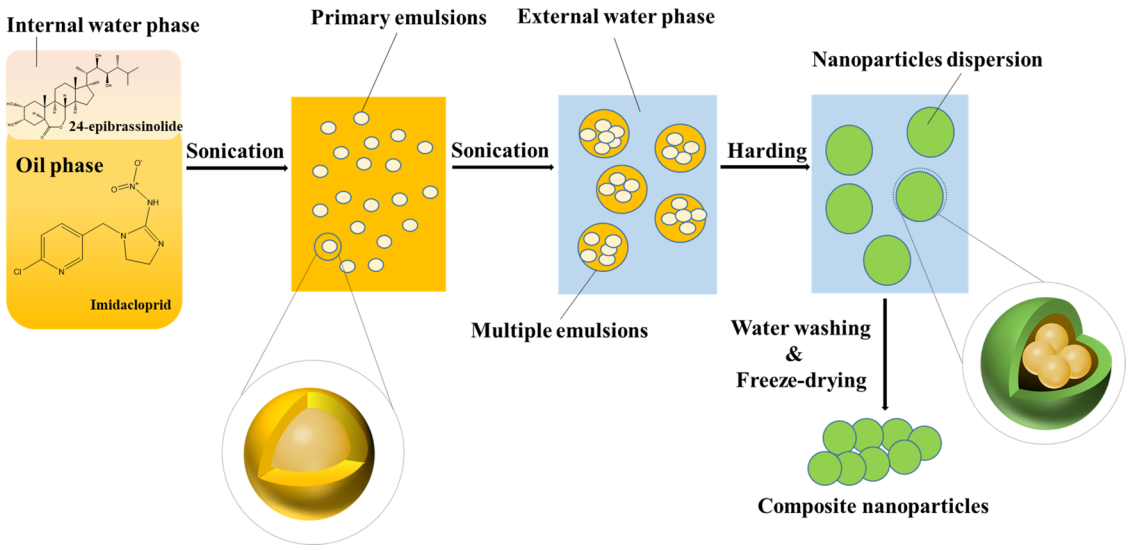

Figure 1. Schematic diagram of the composite nanoparticles preparation process.

residues in agricultural products. At present, there have been a large number of studies on pesticide sustained-release agents to improve the effect of pest control. Kumar et al.[11] synthesized imidacloprid-loaded sodium alginate nanoparticles. The insecticidal activity of the nanoparticles against leafhoppers is more effective than that of normal pesticides. Memarizadeh et al.[12] used poly(citric acid) (PCA) as A block and poly(ethylene glycol) (PEG) as B block to prepare nano-imidacloprid by direct encapsulation of the ABA triblock linear dendrimer, which improved the insecticidal efficiency of imidacloprid. Shang et al.[13] synthesized N-acylated emamectin benzoate by bonding emamectin benzoate with acrylamide. The laboratory toxicity test showed that the efficacy of the new emamectin benzoate preparation against *Helicorvapa armigera* was better than that of emamectin benzoate EC. However, the previous sustained-release pesticide formulations have never been studied on pesticide residues. With the development of the controlled release technique, substances that are conducive to pesticide degradation can be encapsulated in pesticides. Thus, once pesticides complete their mission of pest control, these encapsulated substances will be released to accelerate pesticide degradation and to eliminate the occurrence of pesticide residues from the source. Since the direct degradation agent continuously degrades the pesticide and it is difficult to realize the zero release of the degradation agent before effective pest control, indirect degradation agents are more ideal in the sustained-release formulations to promote pesticide degradation.

Thus, the main objective of the present study was to prepare a new formulation of composite nanoparticles that can enhance pest control efficiency and minimize the residues of the pesticide. Imidacloprid (IMI), a neonicotinoid insecticide, was selected as the studied pesticide, given its high efficiency in piercing−sucking the mouthparts of pests[14] and its low toxicity. As a systemic pesticide, IMI accumulates rapidly in plants, causing toxic symptoms to *Sogatella furcifera* and other insects.[15] 24-Epibrassinolide (24-EBL) accelerates the degradation of residual pesticides by regulating the detoxification system of plants.[15−17] When the 24-EBL content in plants increases, the protease synthesized under the guidance of many genes (such as P450 and GST) can gradually transform pesticides into water-soluble substances or low toxic and nontoxic substances, or even directly exclude them from the body.[18,19] In our proposed composite nanoparticles, 24-EBL was encapsulated in the inner layer, and IMI interacted with the outer-layer wall material of the nanoparticles. We hypothesize that the outer-layer insecticide IMI will be released first to control the *S. furcifera*, and then the internal 24-EBL will be released in the later stage to promote rice growth and degrade the pesticide residues, thus eliminating the occurrence of pesticide residues from the source.

2. MATERIALS AND METHODS

2.1. Materials. IMI (purity 96.2%) was purchased from Jiangsu Fengshan Group Co., Ltd. (Jiangsu, China). 24-EBL (purity 91.6%) was purchased from Zhejiang Shijia Technology Co., Ltd. (Zhejiang, China). Polyhydroxyalkanoate (PHA) was supplied by Changsha Jingkang New Material Technology Co., Ltd. (Changsha, China). Eudragit RS and RL (acrylic resins) (hereafter named as RS/RL) were provided by Shanghai Changwei Pharmaceutical Accessories Technology Co., Ltd. (Shanghai, China). Poly(vinyl alcohol) (PVA-1788, alcoholysis degree: 87.0−89.0% mol/mol) was purchased from Aladdin Industrial Corporation (Shanghai, China). All other reagents were supplied by Sinopharm Chemical Reagent Co., Ltd. Chromatographic methanol and acetonitrile for high-performance liquid chromatography (HPLC) were purchased from Sigma Aloich (Shanghai, China). All chemicals used in the experiments were of analytical grade and used as received without further purification.

2.2. Preparation of IMI and 24-EBL Composite Nanoparticles. The schematic diagram of the preparation process of the proposed composite nanoparticles is shown in Figure 1. The composite nanoparticles were prepared using the W/O/W solvent evaporation technique.[20,21] The 24-EBL (28 mg) was dissolved in acetone (4 mL) and water (3 mL) as the internal water phase. Polymers (RS 32.5 mg/RL 7.5 mg and PHA 112.5 mg) and IMI (150 mg) were dissolved in 5 mL of dichloromethane to form a polymer solution as the oil phase. The 1% (w/V) PVA 1788 solution was the external water phase. One milliliter of the internal water phase was added to 5 mL of the oil phase and sonicated at 67.5 W for 1 min to obtain a primary emulsion (O/W). The primary emulsion was then poured into the external water phase (50 mL) and

https://doi.org/10.1021/acsomega.2c02820
ACS Omega 2022, 7, 29027−29037

sonicated at 195 W for 3 min to obtain a multiple emulsion (W/O/W). Then, the multiple emulsion was placed in a water bath at 40 °C for 30 min for rotary evaporation to remove the solvent dichloromethane and acetone. The nanoparticles dispersion was centrifuged at 10 000 rpm for 10 min, washed with deionized water 3 times, and then freeze dried.

2.3. Extraction and Determination of 24-EBL on HPLC. Because of its unique structure, determination of 24-EBL by HPLC requires a derivatization pretreatment.[22] In this study, phenylboronic acid (PBA) was used for the derivatization of 24-EBL.[23] PBA and 24-EBL, in a certain mass ratio, were dissolved in 20 mL of methanol in a 50 mL volumetric flask and reacted in a water bath at 80 °C until the methanol volatilized completely. Methanol was then added to reach the total volume of 50 mL, followed by sufficient shaking. The experimental designs, including the derivatization strategy of 24-EBL for HPLC analysis and levels of the molar ratio of 24-EBL to PBA, are shown in Supporting Information Part 1.

24-EBL was extracted from the nanoparticles in water and concentrated, since its concentration is below the detection limit. At each concentration, 2.0 mL of 24-EBL was extracted with 3 mL of dichloromethane, followed by removal of the upper aqueous solution. The extracted 24-EBL was dried with N_2 (NDK200-2, Hangzhou Mio Instrument Co., Ltd.) and dissolved in 2 mL of methanol. Then a certain amount of PBA was added for derivatization, under sufficient vortex and mixing. The derivatized 24-EBL was heated in a water bath at 80 °C until the methanol was completely evaporated, and then dissolved in 0.2 mL of methanol. Each treatment was repeated 3 times (see the Supporting Information Part 2 for the details of the HPLC method).

2.4. Characterization of the Composite Nanoparticles. The morphology and size distribution of the composite nanoparticles were observed using a scanning electron microscope (SEM; JSM-6380LV, JEOL, Tokyo, Japan) and transmission electron microscope (TEM; FEI Talos F200S, United States). The material structure analysis was determined using a Fourier transform infrared spectrometer (FTIR; Nicolet-IS 5, United States) and X-ray diffraction (XRD-6000, Shimadzli, Japan). The thermal stability of the nanoparticles was evaluated by thermogravimetric analysis (TGA2, Mettler Toledo, Switzerland).

2.5. In Vitro Release of the Composite Nanoparticles. In order to investigate the release behavior of the composite nanoparticles at different pH and temperatures, freeze-dried nanoparticles (50 mg) were placed in 100 mL of ultrapure water and left to stand for the release process. At pH = 7, the temperature was set to 15, 25, and 35 °C, and the reactors were placed in a temperature-controlled shaking table to allow static release. Then, similar static release experiments were conducted at 25 °C, with the pH set to to 5, 7, and 9. At each specified time interval, 2.5 mL of the supernatant was collected and the same volume of fresh solution was added. From each sample, 2.0 mL was used for the determination of 24-EBL (see section 2.3 for the extraction and derivation of 24-EBL) and 0.5 mL was used to directly determine the content of IMI. The cumulative release rate is calculated as follows

$$\text{cumulative release rate}(\%) = \frac{\text{amount of pesticide released}}{\text{theoretical pesticide amount in nanoparticles}} \times 100\% \quad (1)$$

Several mathematical models were used to evaluate the release mechanism, including zero-order,[24] first-order,[25] Higuchi,[26] and Ritger−Peppas models.[27] Zero-order release equation

$$Q_t = at + b \quad (2)$$

First-order kinetic equation

$$Q_t = a(1 - e^{-bt}) \quad (3)$$

Higuchi equation

$$Q_t = at^{1/2} + b \quad (4)$$

Ritger−Peppas equation

$$Q_t = at^n \quad (5)$$

where Q_t is the cumulative release rate at time t, and a, b, and n are the release rate constants. The diffusion mechanism of the pesticides can be judged according to the value of n. When $n \leq 0.45$, the diffusion of the pesticides follows mainly Fickian diffusion.[27]

2.6. Stability of the Composite Nanoparticles in Light. The stability of the composite nanoparticles was investigated following the method in Xiao et al.[28] Composite nanoparticles (5 mg) were suspended in 10 mL of methanol by ultrasonication. The initial concentration of IMI was 150 mg/L and that of 24-EBL was 2.5 mg/L. IMI and 24-EBL technical with the same concentrations were prepared as controls. Three milliliters of the solution was added into each 10 mL centrifuge tube and a 500 W UV high-pressure mercury lamp was placed 30 cm away from the liquid surface. An independent parallel method was employed in the experiment. One centrifuge tube was removed at each time interval, ten in total. All experiments were repeated 3 times. IMI was directly detected, and 24-EBL was derivatized using PBA and then quantified on HPLC.

2.7. Dissipation of IMI in the Composite Nanoparticles on Rice. The composite nanoparticles were made into a suspending agent (see the Supporting Information Part 3 for details). An indoor pot experiment was carried out with the rice seed "Lingliangyou 211" as the test variety. The recommended dosage (30 mL per acre) of 5% imidacloprid emulsifiable concentrate (IMI EC) was applied and the water consumption was 50 L at the rice seedling stage. 5% IMI EC was taken as control, and 30 mL of each pot was sprayed by the walking spray tower (type 3WP-2000, Nanjing Institute of Agricultural Mechanization, Ministry of Agriculture). The samples and residue testing results were collected at 2 h, 1, 3, 5, 7, 10, 14, and 21 days. The whole plant that grows normally above the soil surface was taken and cut into pieces. After extraction and purification, IMI was detected on HPLC according to the method given in the Supporting Information Part 4 and 5. The dissipation laws were studied according to the dissipation dynamic eq 6 and half-life formulas 7

$$C_T = C_0 \times e^{-kt} \quad (6)$$

$$T_{0.5} = \frac{\text{In } 2}{k} \quad (7)$$

where k is the degradation rate constant, C_0 is the initial concentration of the pesticide, and C_T is the concentration of the pesticide at time t.

At the same time, the effect of 24-EBL in the composite nanoparticles on the growth of rice was studied.[29] Twelve rice seeds with the same bud length were selected and planted in a

https://doi.org/10.1021/acsomega.2c02820
ACS Omega 2022, 7, 29027−29037

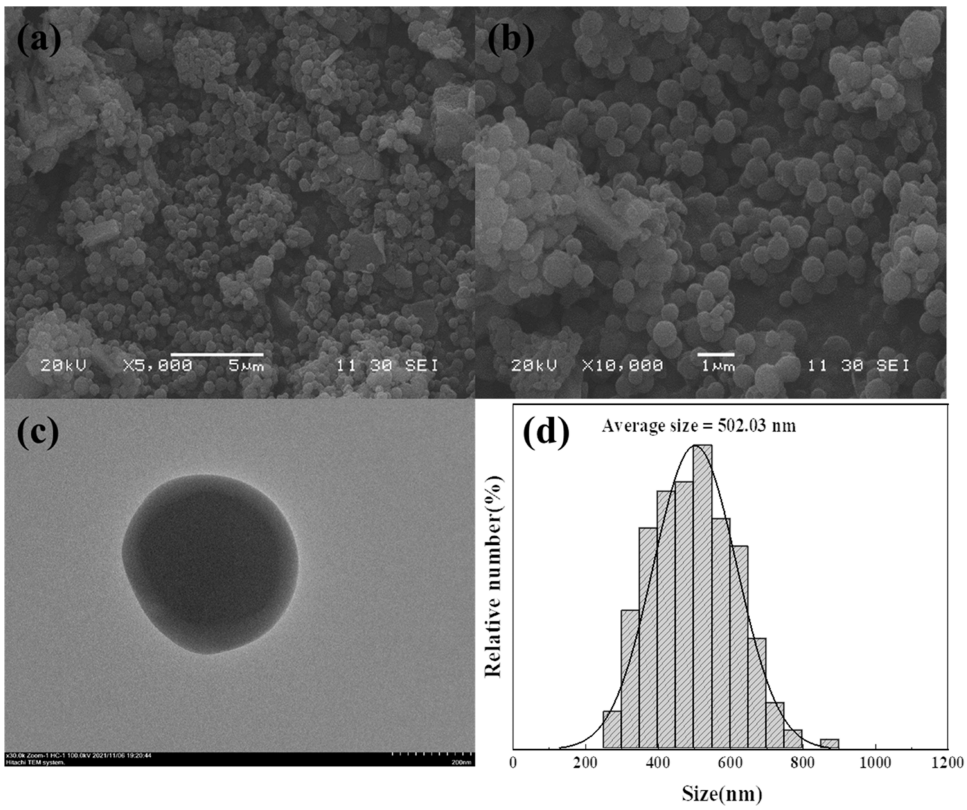

Figure 2. Morphology under SEM (a,b) and TEM (c), and size distributions (d) of the composite nanoparticles.

nutrient bowl, with 5% IMI EC application as the control group. At 7, 14, and 21 days, the plant height, root length, and fresh weight of rice were measured. Each treatment was carried out in triplicate.

2.8. Determination of the Retention and Contact Angle of Composite Nanoparticles on Rice Leaves. The foliar soaking and weighing method was used to determine the foliar retention of composite nanoparticles and 5% IMI EC on rice. Each treatment was conducted 5 times. Pesticide solution was sprayed at the recommended dosage in the field. The leaves were cut into small segments of the same size with a length of 1 cm, and the length and width are measured to calculate the leaf area S (cm^2). A pair of tweezers were put in the experimental pesticide solution in a beaker that was placed on a micro-precision electronic balance, tared to zero. The leaves were thoroughly immersed in the pesticide solution (record the weight W1). The leaves were taken out and weighed (W2) after the pesticide droplets of the leaves were found not dripping. The retention ratio (R_r) of the composite nanoparticle suspension and 5% IMI EC on the leaves was calculated according to formula (8).

$$R_r(\mathrm{mg/cm^2}) = \frac{W1 - W2}{S} \quad (8)$$

Contact angle (CAs) is an important evaluation index to determine the utilization efficiency of the pesticides.[30] Fresh rice leaves were collected without damaging the leaf structure and fixed flat on the stage of the CAs measuring instrument (LAUDA Scientific GmbH, LSA-100). Then, 10 μL droplets of the composite nanoparticle suspension, 5% IMI EC, and water were injected into the rice leaf with a microsyringe. Pictures of the droplets on the leaves were taken at 0, 25, 50, 75, and 100 s to calculate the CAs of the drug solution on the rice.

2.9. Laboratory Toxicity Test. *S. furcifera* was selected as the experimental insect and 5% IMI EC as the control to study the insecticidal activity of composite nanoparticles in the laboratory. Planthoppers were cultured in an artificial climate incubator at a temperature of 27 ± 1 °C and photoperiod light/darkness (L/D) ratio of 14:10. Because the composite nanoparticles in this study have a subsequential process of release and degradation, this experiment will simulate the method of field application rather than the commonly used laboratory toxicity determination method—the rice seedling impregnation method.[31] The sprayed dose was the same as the dissipation of the IMI experiment. In order to verify the duration of the insecticidal activity of the composite nanoparticles 2 h and 7 days after the application of the recommended dose, 20 third instar larvae were placed on each pot of rice, in triplicates. The mortality rate was recorded on the 1st, 2nd, 3rd, and 4th days after the application.

3. RESULTS AND DISCUSSION

3.1. Morphology and Size Distribution of the Composite Nanoparticles. The composite nanoparticles prepared in this study had a uniform spherical shape in the SEM images (Figure 2a,b) and a double-layer structure in the TEM images (Figure 2c). The SEM images also showed adhesion between nanoparticles, which might be due to the agglomeration of nanoparticles caused by intermolecular force.[32] The particle size distribution (Figure 2d) conforms to the normal distribution, with an average particle size of 502.03 ± 114.85 nm. Compared with IMI-controlled release formulation[11,12,20,33] and 24-EBL-controlled release formulation,[34,35] the size of the composite nanoparticles was even smaller than that of some single pesticide nanoparticles.

https://doi.org/10.1021/acsomega.2c02820
ACS Omega 2022, 7, 29027−29037

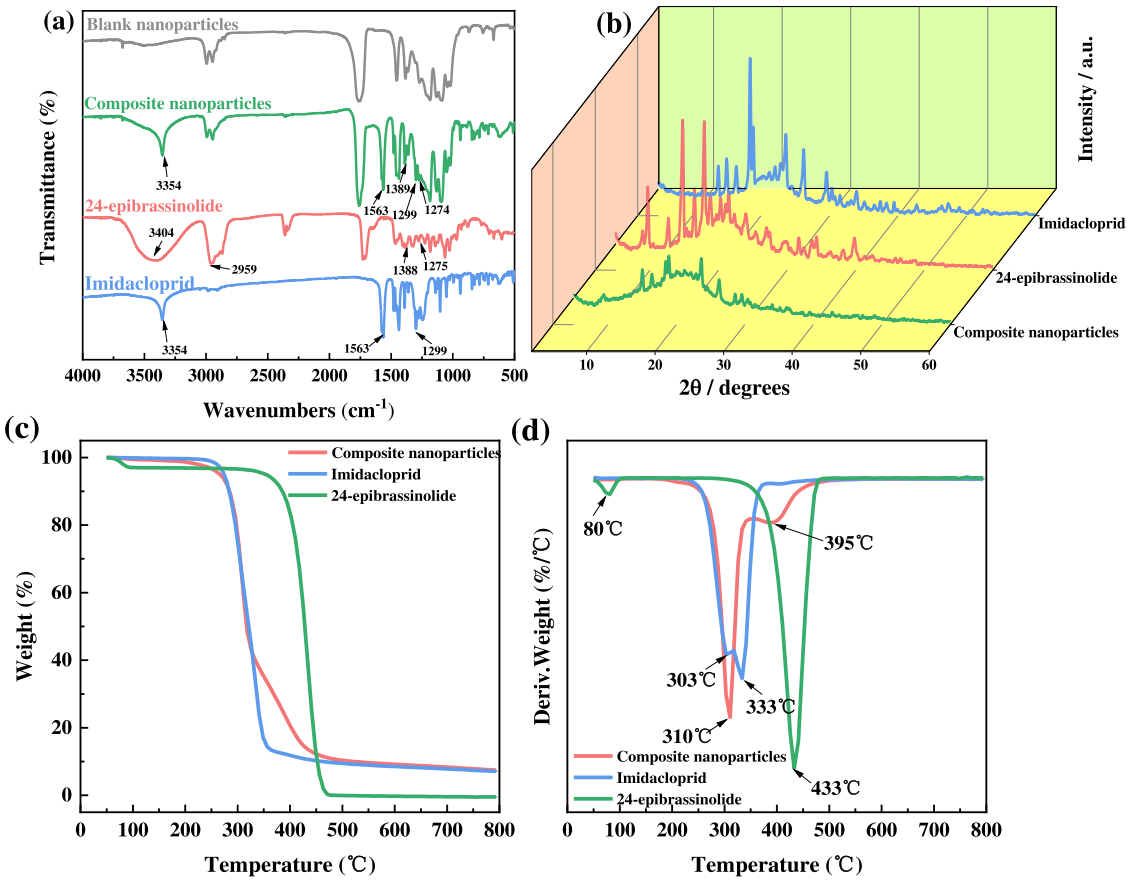

Figure 3. FTIR spectra (a), XRD pattern (b), TGA curve (c), and DTG curve (d) of the composite nanoparticles, IMI, and 24-EBL.

3.2. Characterization of the Composite Nanoparticles. The chemical interactions between blank nanoparticles, composite nanoparticles, IMI, and 24-EBL were investigated using FTIR spectroscopy (Figure 3a). For IMI, the -N-H stretching vibration at 3354 cm^{-1} was the characteristic vibration peak. The absorption peak at 1563 cm^{-1} was the result of the $-NO_2$ stretching vibration. The absorption peaks at 1299 and 1242 cm^{-1} were responsible for the stretching vibration of N−O and C═N, respectively. The FTIR spectra of IMI were consistent with those of Chen et al.[36] and Lim et al.[37] According to the structural formula of 24-EBL, the most important functional group in 24-EBL was -OH, which corresponded to the absorption peak at 3404 cm^{-1} in the FTIR spectrum. The absorption peak at 2959 cm^{-1} was the stretching vibration of $-CH_3$. The absorption peaks of the C−H plane bending vibration at 1388 cm^{-1} and C-O stretching vibration at 1275 cm^{-1} were also observed in the spectrum. The O−H and $-CH_3$ of the 24-EBL may react with the −CO− or R group in the PHA of the wall material. These characteristic absorption peaks of IMI and 24-EBL showed up in the infrared spectrum of the composite nanoparticles, except peaks for the O−H and $-CH_3$ of 24-EBL, which may be the result of the interaction between 24-EBL and the wall material. FTIR analysis indicated that IMI and 24-EBL were successfully loaded.

Besides, X-ray diffraction (XRD) was utilized to analyze the crystal structure of the composite nanoparticles (Figure 3b). For IMI, its characteristic diffraction peaks were at 2θ = 13.68, 14.88, 16.4, 18.46, 23.52, 26.1, 29.56, and 33.98°. The highest peak point (18.46°) was applied in the Scherrer equation to calculate the crystal size, which was 13 nm. This indicated that IMI exists in the crystal structure.[36] The characteristic diffraction peaks of 24-EBL were at 2θ = 9.52, 12.74, 14.9, 16.56, 18.08, 18.88, 20.18, 21.32, 23.82, and 39.66°. 24-EBL had several independent peaks, indicating a high crystallinity. Its highest peak point (14.9°) was applied in the Scherrer equation to calculate the crystal size, which was 0.41 nm. The characteristic diffraction peaks of IMI and 24-EBL were not observed in the nanoparticles, which might indicate that IMI and 24-EBL existed as amorphous structures after interaction with the wall material.[36,38] The crystal size of the composite nanoparticles calculated from the Scherrer equation using the highest peak point (19.56°) was 0.38 nm.

The thermal stability of IMI, 24-EBL, and composite nanoparticles was analyzed through thermogravimetric analysis (TGA) (Figure 3c) and derivative thermogravimetry (DTG) (Figure 3d) in the temperature range of 50−800 °C. For IMI, there were two weight loss stages, which reached the weight loss peaks at 303 and 333 °C, respectively, and IMI began to decompose at 240 °C. When the temperature was increased to 800 °C, the weight loss rate reached 92.91%. The two weight loss stages of 24-EBL were 50−100 and 350−500 °C, respectively. The 2.9% weight loss at the start of the TGA curve of 24-EBL might be due to the evaporation and dehydration of the absorbed and surface water from the material. In the derivative curve, we could easily see that the peak value of weight loss was reached at 433 °C. When the temperature was increased to 487 °C, the weightlessness rate reached 100%. For composite nanoparticles, the first weight loss of 57.16% from 100 to 330 °C, the gradient of which

https://doi.org/10.1021/acsomega.2c02820
ACS Omega 2022, 7, 29027−29037

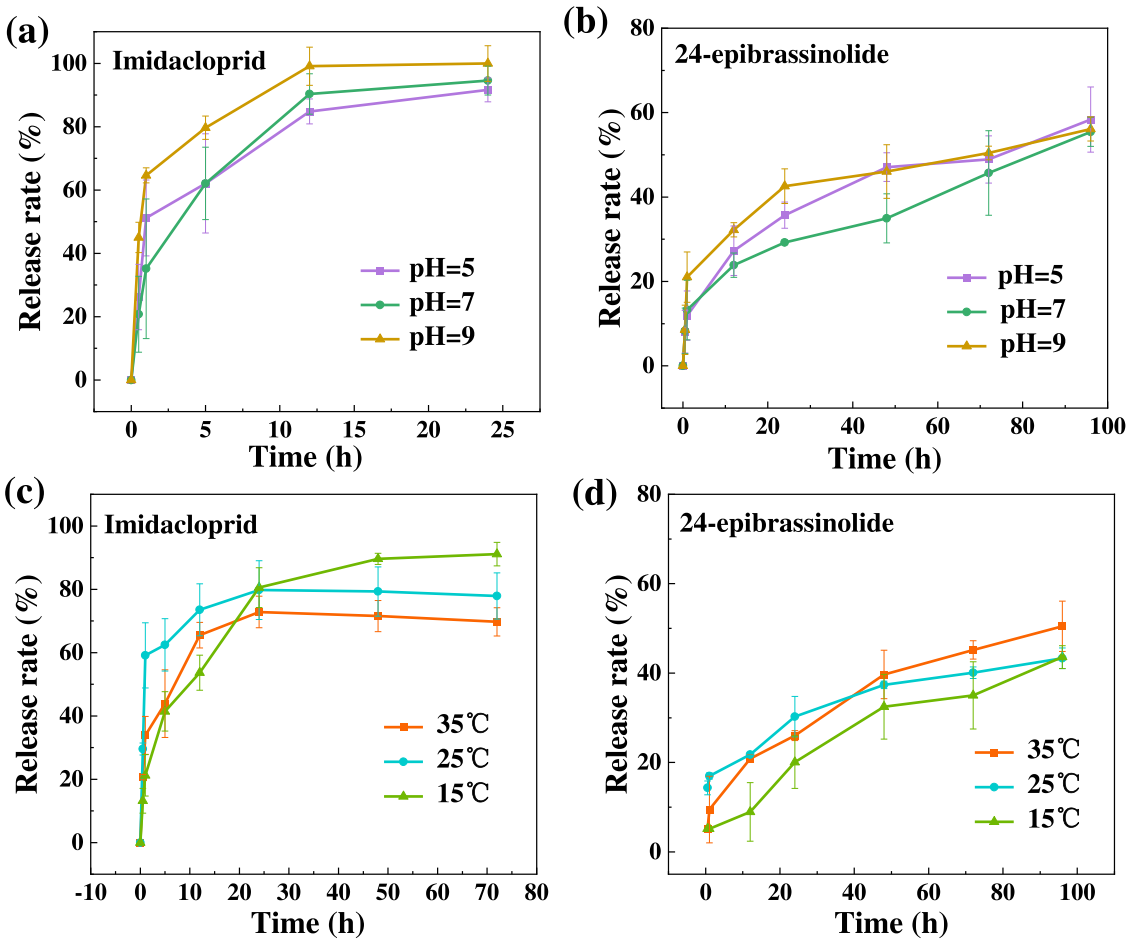

Figure 4. Release behavior of IMI (a) and 24-EBL (b) in water at pH = 5, 7, and 9, and the temporal change of release rate of IMI (c) and 24-EBL (d) at 15, 25, and 35 °C.

peaked at 310 °C, was owing to the decomposition of IMI. The second weight loss of 33.62% from 330 to 550 °C, the gradient of which peaked at 395 °C, was owing to the decomposition of 24-EBL. In composite nanoparticles, the initial maximum decomposition temperature of IMI was delayed from 303 to 310 °C. In addition, the weight loss rate of 24-EBL decreased from 100 to 92.57%. By comparing the TGA and DTG curves, it is reasonable to conclude that composite nanoparticles have better thermal stability.

The structure and stability of the composite nanoparticles determine their effect in practical application. Therefore, composite nanoparticles should have a stable performance to prevent the active ingredient from losing before reaching the target organism.[39] Compared with the traditional formulation, composite nanoparticles can protect the internal effective ingredient and exert efficacy in a specific environment due to the wrapping of the outer wall material.

3.3. Release Behavior of the Composite Nanoparticles. The maximum release rates of the composite nanoparticles at different pH values and temperatures are not significantly different, thus ensuring the wide implication of the composite nanoparticles. At different pH conditions, the maximum release rate of IMI was 90−100% at 24 h and that of 24-EBL was 60% at 96 h (Figure 4a,b). At different temperature conditions, IMI release reached 91% in 72 h at 15 °C, and reached the maximum release of 69−77% in 24 h at 25 and 35 °C; the maximum release rate of 24-EBL was 43−50% within 96 h at 15−35 °C (Figure 4c,d). The composite nanoparticles showed different release amounts under different conditions, but they all showed a similar trend in that IMI was released first and then 24-EBL. Because of its presence on the outer layer of the nanoparticles, IMI was released first, with the maximum release being within 70−100% at 24 h. The release of 24-EBL from the inner layer was slower, and its maximum release was 43−55% at 96 h. Therefore, IMI could be released first to kill insects, and then 24-EBL was released to degrade the pesticide residues of IMI in the later stage.

The encapsulation efficiency (EE) and loading capacity (LC) of IMI and 24-EBL are shown in Table S3. According to the release kinetics equation (Tables S7 and S8), most release equations were in line with the Ritger−Peppas equation, and $n \leq 0.45$, indicating that the release of nanoparticles depended on Fick diffusion. This means that when the pesticide is released in water, it will gradually absorb water and burst to release the pesticide depending on its own permeability.[40] In better control of pests and achieving a good insecticidal effect, the rapid initial release of active ingredients played an important role. It was necessary to have a rapid insecticidal effect to achieve the purpose of long-term pest control.[41] Therefore, the release behavior of the composite nanoparticles will benefit early pest control. Compared with ordinary pesticide microcapsules or nanoparticles, the release was slow[42] or synchronous,[43] and the release of composite nanoparticles in this paper follows the law of sequential

https://doi.org/10.1021/acsomega.2c02820
ACS Omega 2022, 7, 29027−29037

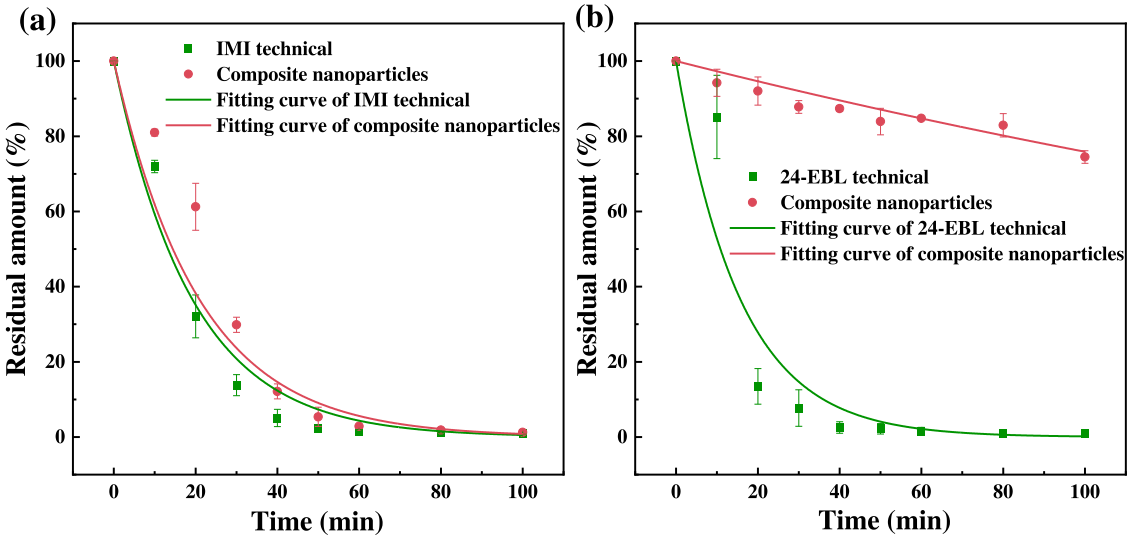

Figure 5. Residual amount of IMI (a) and 24-EBL technical (b), compared with that of composite nanoparticles, under ultraviolet light irradiation. Data are presented as mean±standard deviation (n = 3) and fitted using dissipation dynamic equations.

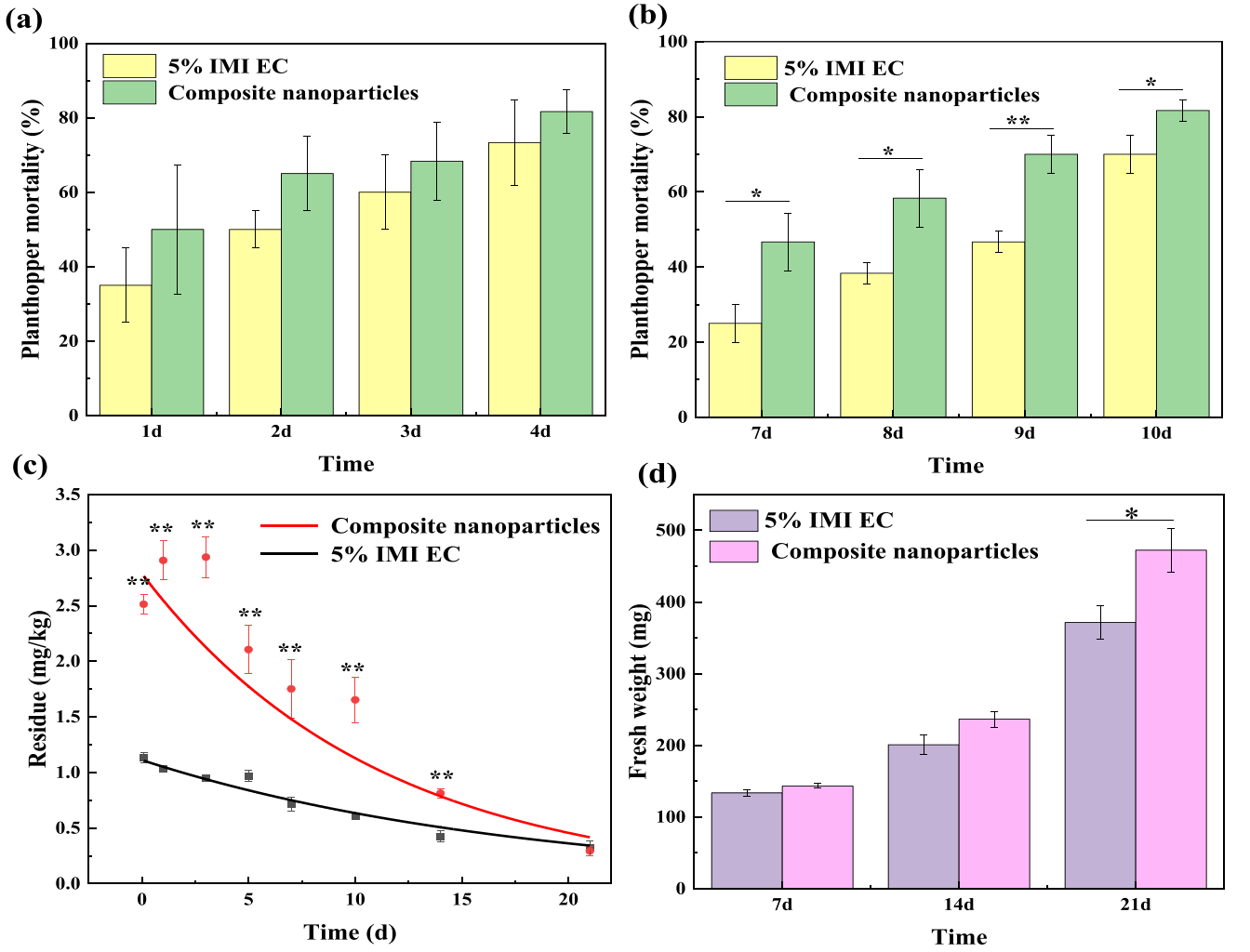

Figure 6. Temporal changes of the death rate of planthoppers 2 h (a) and 7 days (b) after application, (c) IMI residual amount in rice, (d) bioassay, and (e) growth of rice after application of composite nanoparticles versus 5% IMI EC. * Represents a significant difference at 95% confidence level. ** Represents a significant difference at 99% confidence level.

https://doi.org/10.1021/acsomega.2c02820
ACS Omega 2022, 7, 29027−29037

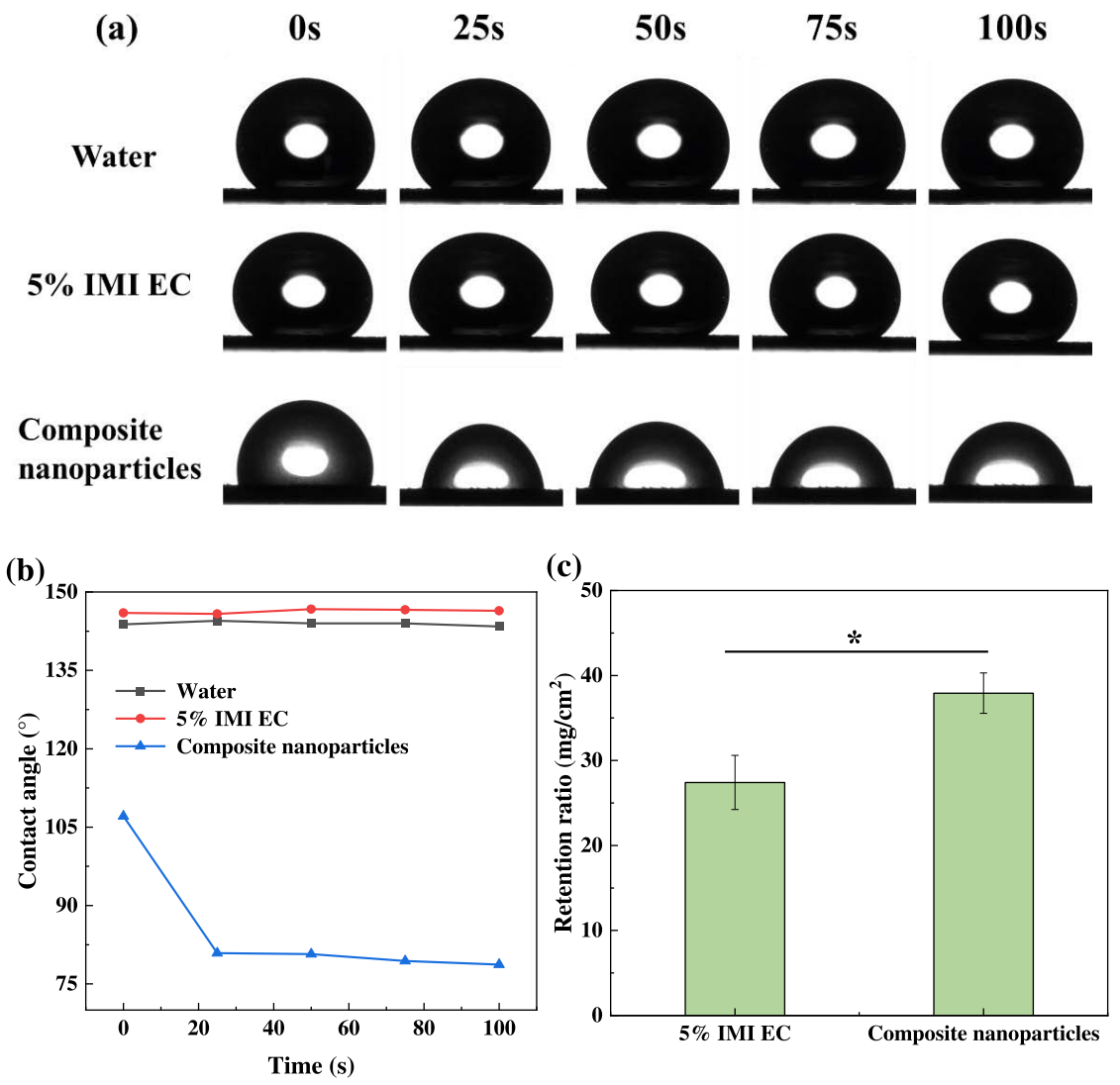

Figure 7. Contact angles against rice (a) and corresponding values (b) within 100 s, and the retention ratio (c) of 5% IMI EC and composite nanoparticles on rice. Error bars indicate standard deviations of replicates (n = 5). * represents a significant difference at 95% confidence level.

release. The research showed that in practical application, the sustained-release preparation could not play a good role, because, in the outbreak period of the pests, the insecticide should achieve the effect of killing the insects quickly, and ensure the validity period to prevent the recurrence of pests. The release of the composite nanoparticles prepared in this study met the different needs of pesticides and plant hormones at the same time. The rapid release of pesticides can ensure the insecticidal rate, while the slow release of plant hormones can promote plant growth and accelerate the degradation of pesticide residues in the later stage, without affecting the efficacy of the insecticides.

3.4. Photodegradation of the Composite Nanoparticles. Improving the photostability of the pesticides was conducive to improving the utilization rate of pesticides and prolonging the duration of effective components.[13] The residual amount of 24-EBL technical increased rapidly with time and only remained 7.72% after 30 min (Figure 5). The 24-EBL degradation ratio of the composite nanoparticles increased slowly and remained 87.8% after 30 min, which indicated that the composite nanoparticles have a higher stability in light. The degradation dynamic equations of IMI, 24-EBL technical, and composite nanoparticles are shown in Table S4. The photolysis half-life of IMI was 13.26 min, and that of IMI in the composite nanoparticles was 14.43 min. The photolysis half-life of 24-EBL was 10.84 min, and that of 24-EBL in the composite nanoparticles was 251.14 min. Under the protection of the wall material, the photodegradation half-lives of IMI and 24-EBL were extended, which was conducive to prolonging the duration of 24-EBL and IMI in light and improving their utilization rate.

3.5. Laboratory Toxicity of IMI to Planthoppers and the Residue on Rice. The laboratory toxicity of the composite nanoparticles is shown in Figure 6a,b. After 7 days, the insecticidal activity of 5% IMI EC decreased, while the composite nanoparticles still maintained the same insecticidal activity as that at 2 h. The toxicity of the composite nanoparticles was higher than that of 5% IMI EC. The mortality of the composite nanoparticles was 81% on the 4th and 10th days, while the mortality of 5% IMI EC was 73 and 70% on the 4th and 10th days, respectively. The insecticidal rates of 5% IMI EC at 1 and 7 days were only 35 and 25%, while the insecticidal rates of composite nanoparticles at 1 and 7 days were 50 and 46%. From day 7,

https://doi.org/10.1021/acsomega.2c02820
ACS Omega 2022, 7, 29027−29037

the insecticidal rate of the composite nanoparticles was significantly higher than that of 5% IMI EC at 95% confidence interval. It showed that the composite nanoparticles had a longer insecticidal duration than 5% IMI EC.

The recoveries and relative standard deviations of IMI on rice are shown in Table S5. Degradation of different concentrations of 24-EBL on the IMI residue in rice was tested (Figure S3 and Table S6). According to the degradation curve (Figure 6c), the amount of composite nanoparticles residue increased at 24 h and 3 days compared to 2 h, indicating a release process of the composite nanoparticles on rice. The degradation rate of composite nanoparticles was lower than that of 5% IMI EC within the initial 10 days, but was faster than EC from 14 days, indicating that the slow-release brassinolide accelerated IMI degradation. Until 21 d, the final residual amount of the composite nanoparticles was equivalent to that of 5% IMI EC. The degradation equation of 5% IMI EC was $y = 1.11e^{-0.056t}$ $R^2 = 0.9615$, with a half-life of $T_{0.5} = 12.37$ days, and that of the composite nanoparticles was $y = 2.79e^{-0.090t}$ $R^2 = 0.9312$, with a half-life of $T_{0.5} = 7.67$ days. The overall degradation half-life was shortened due to the high initial deposition of composite nanoparticles and the faster degradation rate after 14 days. 24-EBL accelerates the degradation of pesticide residues by regulating the detoxification system in plants.[15] Therefore, composite nanoparticles can shorten their half-life and reduce the final residue of the pesticides.

Taking 5% IMI EC as the control, fresh weights were measured at 7, 14, and 21 days after treatment to explore the promoting effect of the composite nanoparticles on rice growth (Figure 6d,e). The plant height and root length are shown in Figure S4. Ten rice plants were collected from each pot for measurement, with 3 repetitions under each treatment. The results showed that composite nanoparticles could promote the growth of rice. There was no significant difference in plant height and root length, but there was a significant difference in fresh weight at 95% confidence level. After 21 days, the composite nanoparticles significantly promoted the increase of fresh weight of rice, whose average value increased from 371 to 472 mg.

3.6. Contact Angle and Adhesion of Composite Nanoparticles on Rice. Rice has hydrophobic leaves,[44] and most pesticides at the recommended dosage levels are difficult to adhere to the rice plant, resulting in the loss of the pesticide and further environmental pollution. Therefore, an enhanced adhesion and wetting ability of the solution on rice can contribute to an improved deposition efficiency of pesticides on rice plants.[45] The contact angles (CAs) of water and 5% IMI EC on rice were 143.8 and 146° at 0 s, respectively, and that of the composite nanoparticles was 107.1° (Figure 7a,b). The CAs of water and emulsion basically did not change at 100 s, while that of the composite nanoparticles gradually decreased to 78.7° at 100 s. The CAs of the composite nanoparticles were about half that of 5% IMI EC, and the initial amount in the pesticide residue experiment was also twice. The contact angle of the composite nanoparticles on rice was smaller than that of 5% IMI EC and water, allowing a better adhesion on rice and higher deposition, which were conducive to the higher efficacy of the pesticides.[28] It showed that the composite nanoparticles can be more absorbed by crops so that the active ingredient can better reach the target organisms to exert their efficacy.

The measurement of leaf retention showed that compared with the commonly used 5% IMI EC (27 mg/cm^2), the deposition amount of composite nanoparticles on rice was higher (37 mg/cm^2), with a significant difference between them (Figure 7c). The deposition efficiency of composite nanoparticles on rice is about 1.4 times that of EC, and the utilization efficiency of pesticides was mentioned to reduce the loss of pesticides. The ratio of the adhesion amount of composite nanoparticles to 5% IMI EC on rice leaves was about 1.4:1, while the initial ratio of pesticide residues was 2:1. The reason for this difference might be that the adhesion amount experiment involved fully extending the leaves into the solution for a few seconds, while in the actual application they were sprayed as small droplets, resulting in the measured adhesion amount of rice leaves in 5% IMI EC being higher than the actual value. Thus, the overall proportional multiple was small.

4. CONCLUSION AND IMPLICATIONS

In this study, a new formulation of composite nanoparticles with aspheric morphology and small particle size (502 nm) was prepared. The continuous release of insecticide IMI in the outer layer of the composite nanoparticles and the increased deposition of IMI on the rice leaves elongate the effective period of pesticides of composite nanoparticles against planthoppers. The subsequent release of 24-EBL accelerates the degradation of IMI on rice, resulting in the IMI residue of the composite nanoparticles at 21 days being equal to that of 5% IMI EC. Common pesticide microcapsules or nanoparticles can also achieve the purpose of elongating the effective period of pesticides through sustained release, whereas the composite nanoparticles in this study further increase the deposition amount on rice by reducing the contact angle of droplets on rice leaves.

However, part of 24-EBL is released in the early stage of the current composite nanoparticles. The wall material of the composite nanoparticles will be adjusted to control the release time of the outer pesticides and the internal substances promoting pesticide degradation to ensure pest control and reduce pesticide residues according to the growth of the crop in further study. At present, detailed analysis on the field application of the controlled release formulation is still lacking.[46] Future research will have to address the behaviors of these composite nanoparticles in actual field conditions and improve their practical properties. Therefore, this research provides a promising way to improve the utilization rate of pesticides and reduce environmental risks, and the new composite nanoparticle formulation has potential application prospects.

■ ASSOCIATED CONTENT

Supporting Information

The Supporting Information is available free of charge at https://pubs.acs.org/doi/10.1021/acsomega.2c02820.

Methods and results; derivatization strategy; derivatization efficiency of 24-EBL; degradation kinetics of IMI; plant growth performance; experimental design for derivertization; recovery rate of 24-EBL; EE and LC of IMI and 24-EBL; degradation dynamics; recovery rate of IMI; temporal changes of IMI residues; release kinetics of IMI and 24-EBL at different pH or temperature conditions (PDF)

https://doi.org/10.1021/acsomega.2c02820
ACS Omega 2022, 7, 29027−29037

AUTHOR INFORMATION

Corresponding Authors

Kailin Liu − *College of Plant Protection, Hunan Agricultural University, Changsha 410128, China; Key Laboratory for Biology and Control of Weeds, Hunan Agricultural Biotechnology Research Institute, Hunan Academy of Agricultural Sciences, Changsha 410125, China;* orcid.org/0000-0002-4830-3137; Email: kailin@hunau.net

Rong Song − *Institute of Agricultural Environment and Ecology, Hunan academy of Agricultural Sciences, Changsha 410125, China*; Email: songrong0205@163.com

Authors

Jingyu Zhao − *College of Plant Protection, Hunan Agricultural University, Changsha 410128, China*

Hui Li − *Department of Crop and Soil Sciences, North Carolina State University, Raleigh, North Carolina 27695, United States;* orcid.org/0000-0002-9374-5305

Qianqi Zheng − *College of Plant Protection, Hunan Agricultural University, Changsha 410128, China*

Shaomei Li − *College of Plant Protection, Hunan Agricultural University, Changsha 410128, China*

Lejun Liu − *College of Plant Protection, Hunan Agricultural University, Changsha 410128, China*

Xiaogang Li − *College of Plant Protection, Hunan Agricultural University, Changsha 410128, China*

Lianyang Bai − *College of Plant Protection, Hunan Agricultural University, Changsha 410128, China; Key Laboratory for Biology and Control of Weeds, Hunan Agricultural Biotechnology Research Institute, Hunan Academy of Agricultural Sciences, Changsha 410125, China*

Complete contact information is available at: https://pubs.acs.org/10.1021/acsomega.2c02820

Notes

The authors declare no competing financial interest.

ACKNOWLEDGMENTS

This work was supported by the Natural Science Foundation of Hunan Province (2021JJ30334), the Science and Technology Plan Projects of Hunan Province (2020SK2033), and the Science Popularization Project of Hunan Province (2021ZK4008).

REFERENCES

(1) Tilman, D.; Fargione, J.; Wolff, B.; et al. Forecasting Agriculturally Driven Global Environmental Change. *Science* **2001**, *292*, 281−284.

(2) McClung, C. R. Making Hunger Yield. *Science* **2014**, *344*, 699−700.

(3) Gunnell, D.; Eddleston, M. Suicide by Intentional Ingestion of Pesticides: A Continuing Tragedy in Developing Countries. *Int. J. Epidemiol.* **2003**, *32*, 902−909.

(4) Pan, X.-l.; Dong, F.; Wu, X.; Xu, J.; Liu, X.; Zheng, Y. Progress of the Discovery, Application, and Control Technologies of Chemical Pesticides in China. *J. Integr. Agric.* **2019**, *18*, 840−853.

(5) Pimentel, D. Amounts of Pesticides Reaching Target Pests: Environmental Impacts and Ethics. *J. Agric. Environ. Ethics* **1995**, *8*, 17−29.

(6) Bollag, J.-M.; Myers, C. J.; Minard, R. D. Biological and Chemical Interactions of Pesticides with Soil Organic Matter. *Sci. Total Environ.* **1992**, *123*−*124*, 205−217.

(7) Li, C.; Zhu, H.; Li, C.; Qian, H.; Yao, W.; Guo, Y. The Present Situation of Pesticide Residues in China and Their Removal and Transformation during Food Processing. *Food Chem.* **2021**, *354*, No. 129552.

(8) Satish, G. P.; Ashokrao, D. M.; Arun, S. K. Microbial Degradation of Pesticide: A Review. *Afr. J. Microbiol. Res.* **2017**, *11*, 992−1012.

(9) Sharma, A.; Kumar, V.; Handa, N.; Bali, S.; Kaur, R.; Khanna, K.; Thukral, A. K.; Bhardwaj, R. Potential of Endophytic Bacteria in Heavy Metal and Pesticide Detoxification. In *Plant Microbiome: Stress Response* Egamberdieva, D.; Ahmad, P., Eds; Microorganisms for Sustainability; Springer Singapore: Singapore, 2018; Vol. 5, pp 307−336.

(10) Li, G.-B.; Wang, J.; Kong, X.-P. Coprecipitation-Based Synchronous Pesticide Encapsulation with Chitosan for Controlled Spinosad Release. *Carbohydr. Polym.* **2020**, *249*, No. 116865.

(11) Kumar, S.; Bhanjana, G.; Sharma, A.; Sidhu, M. C.; Dilbaghi, N. Synthesis, Characterization and on Field Evaluation of Pesticide Loaded Sodium Alginate Nanoparticles. *Carbohydr. Polym.* **2014**, *101*, 1061−1067.

(12) Memarizadeh, N.; Ghadamyari, M.; Adeli, M.; Talebi, K. Preparation, Characterization and Efficiency of Nanoencapsulated Imidacloprid under Laboratory Conditions. *Ecotoxicol. Environ. Saf.* **2014**, *107*, 77−83.

(13) Shang, Q.; Shi, Y.; Zhang, Y.; Zheng, T.; Shi, H. Pesticide-Conjugated Polyacrylate Nanoparticles: Novel Opportunities for Improving the Photostability of Emamectin Benzoate. *Polym. Adv. Technol.* **2013**, *24*, 137−143.

(14) Motaung, T. E. Chloronicotinyl Insecticide Imidacloprid: Agricultural Relevance, Pitfalls and Emerging Opportunities. *Crop Prot.* **2020**, *131*, No. 105097.

(15) Sharma, I.; Bhardwaj, R.; Pati, P. K. Stress Modulation Response of 24-Epibrassinolide against Imidacloprid in an Elite Indica Rice Variety Pusa Basmati-1. *Pestic. Biochem. Physiol.* **2013**, *105*, 144−153.

(16) Zhou, Y. H.; Xia, X. J.; Yu, G.; Wang, J. T.; Wu, J. X.; Wang, M. M.; Yang, Y. X.; Shi, K.; Yu, Y. L.; Chen, Z. X.; et al. Brassinosteroids Play a Critical Role in the Regulation of Pesticide Metabolism in Crop Plants. *Sci. Rep.* **2015**, *5*, No. 9018.

(17) Xia, X. J.; Zhang, Y.; Wu, J. X.; Wang, J. T.; Zhou, Y. H.; Shi, K.; Yu, Y. L.; Yu, J. Q. Brassinosteroids Promote Metabolism of Pesticides in Cucumber. *J. Agric. Food Chem.* **2009**, *57*, 8406−8413.

(18) Hou, J.; Zhang, Q.; Zhou, Y.; Ahammed, G. J.; Zhou, Y.; Yu, J.; Fang, H.; Xia, X. Glutaredoxin GRXS16 Mediates Brassinosteroid-Induced Apoplastic H_2O_2 Production to Promote Pesticide Metabolism in Tomato. *Environ. Pollut.* **2018**, *240*, 227−234.

(19) Hou, J.; Sun, Q.; Li, J.; Ahammed, G. J.; Yu, J.; Fang, H.; Xia, X. Glutaredoxin S25 and Its Interacting TGACG Motif-Binding Factor TGA2 Mediate Brassinosteroid-Induced Chlorothalonil Metabolism in Tomato Plants. *Environ. Pollut.* **2019**, *255*, No. 113256.

(20) Zheng, Q.; Niu, Y.; Li, H. Synthesis and Characterization of Imidacloprid Microspheres for Controlled Drug Release Study. *React. Funct. Polym.* **2016**, *106*, 99−104.

(21) Coombes, A. G. A.; Yeh, M.-K.; Lavelle, E. C.; Davis, S. S. The Control of Protein Release from Poly(Dl-Lactide Co-Glycolide) Microparticles by Variation of the External Aqueous Phase Surfactant in the Water-in Oil-in Water Method. *J. Controlled Release* **1998**, *52*, 311−320.

(22) Sasse, J. M. Recent Progress in Brassinosteroid Research. *Physiol. Plant.* **1997**, *100*, 696−701.

(23) Gamoh, K.; Yamaguchi, I.; Takatsuto, S.; et al. Rapid and Selective Sample Preparation for the Chromatographic Determination of Brassinosteroids from Plant Material Using Solid-Phase Extraction Method. *Anal. Sci.* **1994**, *10*, 913−917.

(24) Costa, P.; Sousa Lobo, J. M. Modeling and Comparison of Dissolution Profiles. *Eur. J. Pharm. Sci.* **2001**, *13*, 123−133.

(25) England, C. G.; Miller, M. C.; Kuttan, A.; Trent, J. O.; Frieboes, H. B. Release Kinetics of Paclitaxel and Cisplatin from Two and

https://doi.org/10.1021/acsomega.2c02820
ACS Omega 2022, 7, 29027−29037

Three Layered Gold Nanoparticles. *Eur. J. Pharm. Biopharm.* **2015**, *92*, 120−129.
(26) Higuchi, T. Rate of Release of Medicaments from Ointment Bases Containing Drugs in Suspension. *J. Pharm. Sci.* **1961**, *50*, 874−875.
(27) Ritger, P. L.; Peppas, N. A. A Simple Equation for Description of Solute Release II. Fickian and Anomalous Release from Swellable Devices. *J. Controlled Release* **1987**, *5*, 37−42.
(28) Xiao, D.; Liang, W.; Xie, Z.; Cheng, J.; Du, Y.; Zhao, J. A Temperature-Responsive Release Cellulose-Based Microcapsule Loaded with Chlorpyrifos for Sustainable Pest Control. *J. Hazard. Mater.* **2021**, *403*, No. 123654.
(29) Chon, N. M.; Nishikawa-koseki, N.; Hirata, Y.; Saka, H.; Abe, H. Effects of Brassinolide on Mesocotyl, Coleoptile and Leaf Growth in Rice Seedlings. *Plant Prod. Sci.* **2000**, *3*, 360−365.
(30) Song, Y.; Huang, G.; Zheng, L.; Huang, Q.; Cao, L.; Li, F.; Zhao, P.; Zhang, L.; Cao, C. Polymer Additives Regulate the Deposition Behavior of Pesticide Droplets on Target Plants. *Polym. Test.* **2021**, *93*, No. 106958.
(31) Nauen, R.; Ebbinghaus-Kintscher, U.; Salgado, V. L.; Kaussmann, M. Thiamethoxam Is a Neonicotinoid Precursor Converted to Clothianidin in Insects and Plants. *Pestic. Biochem. Physiol.* **2003**, *76*, 55−69.
(32) Zare, Y. Study of Nanoparticles Aggregation/Agglomeration in Polymer Particulate Nanocomposites by Mechanical Properties. *Composites, Part A* **2016**, *84*, 158−164.
(33) Guan, H.; Chi, D.; Yu, J.; Li, X. A Novel Photodegradable Insecticide: Preparation, Characterization and Properties Evaluation of Nano-Imidacloprid. *Pestic. Biochem. Physiol.* **2008**, *92*, 83−91.
(34) Quiñones, J. P.; García, Y. C.; Curiel, H.; Covas, C. P. Microspheres of Chitosan for Controlled Delivery of Brassinosteroids with Biological Activity as Agrochemicals. *Carbohydr. Polym.* **2010**, *80*, 915−921.
(35) Pérez Quiñones, J.; Brüggemann, O.; Kjems, J.; Shahavi, M. H.; Peniche Covas, C. Novel Brassinosteroid-Modified Polyethylene Glycol Micelles for Controlled Release of Agrochemicals. *J. Agric. Food Chem.* **2018**, *66*, 1612−1619.
(36) Chen, M.; Wang, J.; Zhang, W.; Diao, G. Preparation and Characterization Water-Soluble Inclusion Complexes of Imidacloprid-*β*-Cyclodextrin Polymer and Their Electrochemical Behavior. *J. Electroanal. Chem.* **2013**, *696*, 1−8.
(37) Lim, G.-P.; Ahmad, M. S. Development of Ca-Alginate-Chitosan Microcapsules for Encapsulation and Controlled Release of Imidacloprid to Control Dengue Outbreaks. *J. Ind. Eng. Chem.* **2017**, *56*, 382−393.
(38) Naghizadeh, M.; Taher, M. A.; Tamaddon, A.-M. Facile Synthesis and Characterization of Magnetic Nanocomposite ZnO/$CoFe_2O_4$ Hetero-Structure for Rapid Photocatalytic Degradation of Imidacloprid. *Heliyon* **2019**, *5*, No. e02870.
(39) Christian, P.; Von der Kammer, F.; Baalousha, M.; Hofmann, Th. Nanoparticles: Structure, Properties, Preparation and Behaviour in Environmental Media. *Ecotoxicology* **2008**, *17*, 326−343.
(40) Piras, A. M.; Sandreschi, S.; Maisetta, G.; Esin, S.; Batoni, G.; Chiellini, F. Chitosan Nanoparticles for the Linear Release of Model Cationic Peptide. *Pharm. Res.* **2015**, *32*, 2259−2265.
(41) Luo, J.; Zhang, D.; Jing, T.; Liu, G.; Cao, H.; Li, B.; Hou, Y.; Liu, F. Pyraclostrobin Loaded Lignin-Modified Nanocapsules: Delivery Efficiency Enhancement in Soil Improved Control Efficacy on Tomato Fusarium Crown and Root Rot. *Chem. Eng. J.* **2020**, *394*, No. 124854.
(42) Cao, L.; Liu, Y.; Xu, C.; Zhou, Z.; Zhao, P.; Niu, S.; Huang, Q. Biodegradable Poly(3-Hydroxybutyrate-Co-4-Hydroxybutyrate) Microcapsules for Controlled Release of Trifluralin with Improved Photostability and Herbicidal Activity. *Mater. Sci. Eng. C* **2019**, *102*, 134−141.
(43) Wang, Y.; Li, C.; Wang, Y.; Zhang, Y.; Li, X. Compound Pesticide Controlled Release System Based on the Mixture of Poly(Butylene Succinate) and PLA. *J. Microencapsulation* **2018**, *35*, 494−503.
(44) Kurokawa, Y.; Nagai, K.; Huan, P. D.; Shimazaki, K.; et al. Rice Leaf Hydrophobicity and Gas Films Are Conferred by a Wax Synthesis Gene (LGF1) and Contribute to Flood Tolerance. *New Phytol.* **2018**, *218*, 1558−1569.
(45) Wei, J.; Tang, Y.; Wang, M.; Hua, G.; Zhang, Y.; Peng, R. Wettability on Plant Leaf Surfaces and Its Effect on Pesticide Efficiency. *Int. J. Precis. Agric. Aviat.* **2018**, *1*, 30−37.
(46) Kah, M.; Kookana, R. S.; Gogos, A.; Bucheli, T. D. A Critical Evaluation of Nanopesticides and Nanofertilizers against Their Conventional Analogues. *Nat. Nanotechnol.* **2018**, *13*, 677−684.

https://doi.org/10.1021/acsomega.2c02820
ACS Omega 2022, 7, 29027−29037